

Very Long-chain Fatty Acid-containing Lipids rather than Sphingolipids *per se* Are Required for Raft Association and Stable Surface Transport of Newly Synthesized Plasma Membrane ATPase in Yeast*

Barbara Gaigg, Alexandre Toulmay, and Roger Schneider¹

From the Division of Biochemistry, University of Fribourg, CH-1700 Fribourg, Switzerland

The proton-pumping H⁺-ATPase, Pma1p, is an abundant and very long lived polytopic protein of the yeast plasma membrane. Pma1p constitutes a major cargo of the secretory pathway and thus serves as a model to study plasma membrane biogenesis. Pma1p associates with detergent-resistant membrane domains (lipid “rafts”) already in the ER, and a lack of raft association correlates with mistargeting of the protein to the vacuole, where it is degraded. We are analyzing the role of specific lipids in membrane domain formation and have previously shown that surface transport of Pma1p is independent of newly synthesized sterols but that sphingolipids with C26 very long chain fatty acid are crucial for raft association and surface transport of Pma1p (Gaigg, B., Timischl, B., Corbino, L., and Schneider, R. (2005) *J. Biol. Chem.* 280, 22515–22522). We now describe a more detailed analysis of the function that sphingolipids play in this process. Using a yeast strain in which the essential function of sphingolipids is substituted by glycerophospholipids containing C26 very long chain fatty acids, we find that sphingolipids *per se* are dispensable for raft association and surface delivery of Pma1p but that the C26 fatty acid is crucial. We thus conclude that the essential function of sphingolipids for membrane domain formation and stable surface delivery of Pma1p is provided by the C26 fatty acid that forms part of the yeast ceramide.

Integral membrane proteins enter the membrane environment in the ER² and are then transported along a vesicular pathway to their final subcellular destination (1). Although much attention has been paid to uncovering the role of protein-encoded signals in determining sorting of the membrane-bound cargo to its final destination, comparatively little is known about how the lipid-protein interface itself affects protein sorting. The integrity of this interface is probably surveilled by components of the protein quality control system to ensure that only functional proteins are delivered to the cell surface

when needed. Co-delivery of integral membrane proteins together with their surrounding membrane domain to the cell surface may, in principle, ensure balanced expansion of the plasma membrane itself.

The proton-pumping H⁺-ATPase, Pma1p, is biosynthetically inserted into the ER membrane, where it homo-oligomerizes to form a 1.8-MDa complex that resists detergent extraction (2). This complex is then packaged into a larger subclass of COPII transport vesicles that contain Lst1p in addition to Sec24p (3) and is transported to the cell surface by a branch of the secretory pathway that does not intersect with endosomes (4, 5). Once at surface, Pma1p becomes stabilized and occupies domains that are distinct from those occupied by the arginine/H⁺ symporter Can1p (6).

A relationship between Pma1p biogenesis and lipid synthesis is indicated by the observations that long-chain base or ceramide synthesis is required for oligomerization and raft association of Pma1p in the ER (2, 7). Oligomerization of Pma1p, however, is not required for ER export or surface delivery but might be important for stabilization of the protein at the cell surface (2, 7). Raft association of Pma1p, on the other hand, is required for surface delivery and subsequent stabilization of the protein (7–9).

We previously observed that newly synthesized Pma1p is mistargeted to the vacuole in an *elo3Δ* mutant that affects acyl chain elongation and hence the synthesis of the ceramide-bound C26 very long-chain fatty acid (10). Further characterization of the role of lipids in Pma1p biogenesis revealed that neither sterols nor the head group modifications on the sphingolipids are important for raft association and surface transport of Pma1p (11). Instead, the results suggested that ceramide levels and/or their substitution with saturated very long-chain fatty acids are crucial for the biogenesis of Pma1p. These results also indicated that the lipid requirement of Pma1p to form membrane microdomains is distinct from the classical sterol and sphingolipid-rich domains that are normally referred to as detergent-resistant membranes/lipid rafts (12–14).

The aim of this study is to discriminate between the role of ceramide and that of the very long-chain fatty acid in Pma1p sorting. Such discrimination is made possible by the use of a mutant that bypasses the essential requirement for sphingolipids by producing unusual inositol-containing glycerophospholipids carrying a C26 fatty acid in the *sn*-2 position (15). Surprisingly, Pma1p is raft-associated and stably transported to the cell

* This work was supported by Swiss National Science Foundation Grant 631-065925. The costs of publication of this article were defrayed in part by the payment of page charges. This article must therefore be hereby marked “advertisement” in accordance with 18 U.S.C. Section 1734 solely to indicate this fact.

¹ To whom correspondence should be addressed: Dept. of Medicine, Division of Biochemistry, University of Fribourg, Chemin du Musée 5, CH-1700 Fribourg. Tel.: 41-26-300-8654; Fax: 41-26-300-9735; E-mail: roger.schneider@unifr.ch.

² The abbreviations used are: ER, endoplasmic reticulum; PHS, phytosphingosine; GFP, green fluorescent protein.

TABLE 1

S. cerevisiae strains used in this study

Strain	Relevant genotype	Source or reference
YRS1878	<i>MATa ura3-52 leu2-3,112 ade1</i>	22
YRS1877	<i>MATa ura3-52 leu2-3,112 ade1 lcb1::URA3 SLC1-1</i>	22
YRS1029	<i>MATa ura3 leu2 his4 bar1 end8-1</i>	49
YRS1118	<i>MATα his3Δ200 leu2Δ1 ura3-52 elo3::his5</i>	10
YRS2915	<i>MATa ura3-52 leu2-3,112 ade1 pep4::LEU2</i>	This work
YRS2138	<i>MATa ura3-52 leu2-3,112 ade1 lcb1::URA3 SLC1-1 pep4::LEU2</i>	This work
YRS2569	<i>MATa ura3-52 leu2-3,112 ade1 p[PMA-GFP-URA3]</i>	This work
YRS2942	<i>MATa ura3-52 leu2-3,112 ade1 lcb1::URA3 SLC1-1 p[PMA1-GFP-LEU2]</i>	This work
YRS2914	<i>MATa ura3-52 leu2-3,112 ade1 lcb1::URA3 SLC1-1 elo3::kanMX4</i>	This work
YRS2943	<i>MATa ura3-52 leu2-3,112 ade1 lcb1::URA3 SLC1-1 elo3::kanMX4 p[PMA1-GFP-LEU2]</i>	This work

surface if sphingolipids are replaced by C26-containing glycerophospholipids. Reduction of the length of the acyl chain on the suppressor lipids, however, impairs the essential function of these lipids and results in conditional degradation of Pma1p, strongly indicating that lipids with a C26 fatty acid either bound to a glycerophospholipid or to ceramide are crucial for the vital function of sphingolipids and for surface delivery and stability of Pma1p. These observations are discussed in the context of a possible hydrophobic match between the length of a protein transmembrane domain and the thickness of its surrounding lipid membrane as a parameter that may affect Pma1p sorting to or retention at the plasma membrane of yeast.

EXPERIMENTAL PROCEDURES

Yeast Strains and Growth Conditions—Yeast strains used in this study are listed in Table 1. Strains bearing single deletions of nonessential genes were obtained from EUROSCARF (available on the World Wide Web at www.rz.uni-frankfurt.de/FB/fb16/mikro/euroscarf/index.html) (16). Strains were cultivated at 24, 30, or 37 °C in YPD-rich medium (1% Bacto yeast extract, 2% Bacto peptone (USBiological, Swampscott, MA), 2% glucose) or in minimal medium. Cells lacking sphingolipids were cultivated in complete synthetic medium or complete complex medium as described (17). Phytosphingosine (PHS) was supplemented in 0.5% Tergitol at a concentration of 25 μM. The presence of the kanMX marker was selected for by growing the cells on medium containing 200 μg/ml G418 (Invitrogen). Chemicals were purchased from Sigma, unless otherwise noted. Aureobasidin A was obtained from Takara Bio Inc. (Shiga, Japan); myriocin and fumonisins B1 were from Alexis Corp. (Lausen, Switzerland).

For DNA cloning and propagation of plasmids, *Escherichia coli* strain XL1-blue (Stratagene, La Jolla, CA) was used. To generate double mutants with *pep4Δ*, a *pep4::LEU2* disruption cassette (pTS17; Tom Stevens, University of Oregon, Eugene, OR) was cut with BamHI and used for transformation. *PEP4* disruption was confirmed by PCR and a plate assay for carboxypeptidase Y activity.

The plasmid containing a GFP-tagged version of Pma1p was kindly provided by A. Breton (Institut de Biochimie et Genetique Cellulaires, Bordeaux, France) (18). The *URA3* marker on this plasmid was switched to *LEU2* using the marker swap plasmid pUL9 (19).

Isolation of Detergent-insoluble Membrane Domains—Detergent-insoluble membrane domains were isolated after flotation on Optiprep gradients (Axis-Shield, Huntingdon, UK) as previously described (10, 20). Proteins were precipitated with

trichloroacetic acid (10%), dissolved in sample buffer, and subjected to SDS-PAGE and Western blot analyses using rabbit antibodies against Pma1p (1:10,000), Gas1p (1:2000; a kind gift from A. Conzelmann, University Fribourg, Switzerland), and Wbp1p (1:1000; a kind gift from C. Jakob and M. Aebi, ETH Zurich, Switzerland).

Pulse-Chase Analysis—For pulse-chase analysis, cells were grown to $A_{600\text{ nm}} \sim 1$ in minimal medium lacking cysteine and methionine, unless otherwise noted, and the culture was then split and preincubated at either 24 or 37 °C for 15 min. Cells were pulsed with 100 μCi/ml EXPRE^{35S} protein labeling mix (~1175 Ci/mmol; PerkinElmer Life Sciences) for 5 min. Chase was initiated by the addition of chase solution (100×; 0.3% cysteine, 0.3% methionine, 300 mM ammonium sulfate). At each time point, cells were removed (1 $A_{600\text{ nm}}$ unit), placed on ice, and arrested with 20 mM Na₃N₃/NaF. Cells were centrifuged; resuspended in 50 mM Tris-HCl, pH 7.5, 5 mM EDTA, 10 μg/ml leupeptin A, 10 μg/ml pepstatin; and disrupted by vortexing with glass beads. SDS was added to 1%, and the lysate was incubated at 45 °C for 10 min. The lysate was diluted by the addition of 800 μl of TNET (30 mM Tris-HCl, pH 7.5, 120 mM NaCl, 5 mM EDTA, 1% Triton X-100) and centrifuged at 15,000 × *g* for 10 min. The supernatant was incubated with anti-Pma1p antibody and protein A-Sepharose. Immunoprecipitates were analyzed by SDS-PAGE, visualized with a PhosphorImager, and quantified using Quantify One software (Bio-Rad).

Detergent resistance of newly synthesized Pma1p was examined as previously described (9–11). Lysates of labeled cells (3–4 $A_{600\text{ nm}}$ equivalents) were extracted with 1% Triton X-100 for 30 min at 4 °C. Samples were centrifuged at 100,000 × *g* for 1 h. Pellets were resuspended in 1% SDS. Detergent concentrations in aliquots of total, supernatant, and pellet samples were adjusted for immunoprecipitation.

Fluorescence Microscopy—*in vivo* localization of green fluorescent protein (GFP)-tagged Pma1p was performed by fluorescence microscopy using a Zeiss Axioplan 2 microscope (Carl Zeiss, Oberkochen, Germany) equipped with an AxioCam CCD camera and AxioVision 3.1 software. Lucifer yellow uptake was examined as described (21).

Lipid Analysis—For sphingolipid analysis, 10 $A_{600\text{ nm}}$ units of cells (1×10^8 cells) grown in SC-inositol were harvested, resuspended in 1 ml of fresh SC-inositol, and labeled by the addition of 40 μCi of [³H]inositol (1 mCi/ml; American Radiolabeled Chemicals Inc., St. Louis, MO). Cells were incubated for 40 min at 30 °C, diluted with prewarmed fresh medium, and incubated

for another 80 min. Labeling was terminated by adding NaF and NaN₃ to a final concentration of 20 mM. Cells were harvested and broken with glass beads, and lipids were extracted with chloroform/methanol (1:1; v/v). Phospholipids were deacylated by treatment with mild base, and sphingolipids were analyzed by thin layer chromatography on silica gel 60 plates (Merck) using chloroform, methanol, 0.25% KCl (55:45:5; v/v/v) as the solvent system. Radioactivity was detected and quantified by two-dimensional radioscanning on a Berthold Tracemaster 40, and plates were visualized using a PhosphorImager (Bio-Rad).

For lipid analysis by mass spectrometry, 40,000 × g microsomal membranes were extracted three times with ethanol/water/diethylether/pyridine/NH₄OH (15:15:5:1:0.018; v/v/v/v/v) at 60 °C, for 15 min each. Lipids were resuspended in chloroform/methanol (1:1; v/v) and analyzed in the negative ion mode on a Bruker Esquire HCT ion trap mass spectrometer (ESI) with a flow rate of 120 μl/h and a capillary tension of −250 V. Ion fragmentation was induced with argon as collision gas at a pressure of 8 millibars.

RESULTS

Characterization of the *SLC1-1* Suppressor Strain—Sphingolipids or intermediates of the sphingolipid biosynthetic pathway are essential lipids in yeast, as indicated by the fact that long-chain base synthesis mediated by serine palmitoyltransferase (*LCB1,2*) is vital (22, 23). However, the essential requirement for long-chain base synthesis is bypassed in a suppressor strain that produces novel C26 fatty acid-containing inositol glycerophospholipids that structurally mimic sphingolipids (Fig. 1) (15). The semidominant *SLC1-1* mutation results in a Q44L substitution in Slc1p, an 1-acyl-*sn*-glycerol-3-phosphate acyltransferase (24). The semidominant mutation is thus thought to confer altered substrate specificity to Slc1-1p, enabling the transfer of C26 to the *sn*-2 position of glycerophospholipids (24).

To determine the relative fitness of the *SLC1-1* suppressor strain, we first analyzed its growth and viability in the presence or absence of exogenous phytosphingosine (PHS) as a long-chain base that restores sphingolipid synthesis in this strain (Fig. 2, A and B). This analysis revealed that the *SLC1-1* strain grew more slowly than a corresponding wild-type strain but that the strain remained fully viable even in the absence of PHS. PHS itself did not appear to significantly improve growth of the suppressor strain but inhibited growth of both *SLC1-1* and wild-type cells. Labeling of cells with [³H]inositol confirmed the absence of sphingolipids, since there were no detectable mild base-resistant lipids present in *SLC1-1* when grown without PHS. The addition of PHS, however, restored sphingolipid synthesis in the suppressor strain (Fig. 2C).

The presence of C26-containing inositol glycerophospholipids in *SLC1-1* was furthermore confirmed by mass spectrometry, which revealed two major C26-containing inositol glycerophospholipid species in *SLC1-1* that were not detectable in wild-type cells (Fig. 2D). Presence of the C26 fatty acid in these two lipid species was confirmed by collision induced fragmentation, which yielded an ion of *m/z* 395, characteristic for C26 (Fig. 2E).

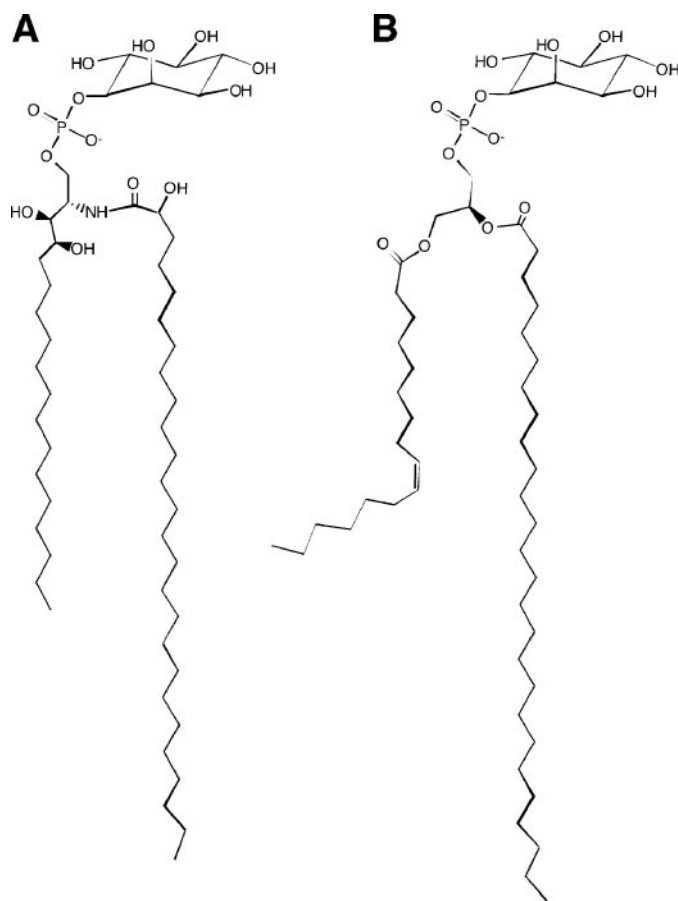


FIGURE 1. Structural comparison of sphingolipids and C26-containing inositol glycerophospholipids made in the *SLC1-1* strain. A, structure of a yeast sphingolipid, inositolphosphorylceramide, containing ceramide with an amide-linked C26 very long-chain fatty acid. B, structure of a suppressor lipid containing a C26 fatty acid in *sn*-2 position of an inositol glycerophospholipid.

Taken together, these results indicate that the *SLC1-1* strain is viable in the absence of sphingolipids and that the strain synthesizes C26-containing inositol glycerophospholipids, consistent with the original characterization of the lipids made by the suppressor strain (15).

Association of *Pma1p* and *Gas1p* with Detergent-resistant Membranes in the Absence of Sphingolipids—We next examined whether the association of plasma membrane proteins with detergent-resistant membranes was affected by the absence of sphingolipids in *SLC1-1*. The glycosylphosphatidylinositol-anchored *Gas1p* and the polytopic proton-pumping ATPase *Pma1p* are two yeast plasma membrane proteins that associate with detergent-resistant membranes (20). Steady-state association of these two proteins with detergent-resistant membranes depends on sphingolipids and sterols (20). To examine raft association of *Gas1p* and *Pma1p* in cells lacking sphingolipids, membranes were prepared from wild-type and *SLC1-1* cells that were grown in the presence or absence of PHS. These membranes were then extracted with detergent and floated in an Optiprep density gradient to separate detergent-resistant membranes in the top fractions of the gradient from the solubilized material. This analysis revealed that *Pma1p* and *Gas1p* were both enriched in the detergent-resis-

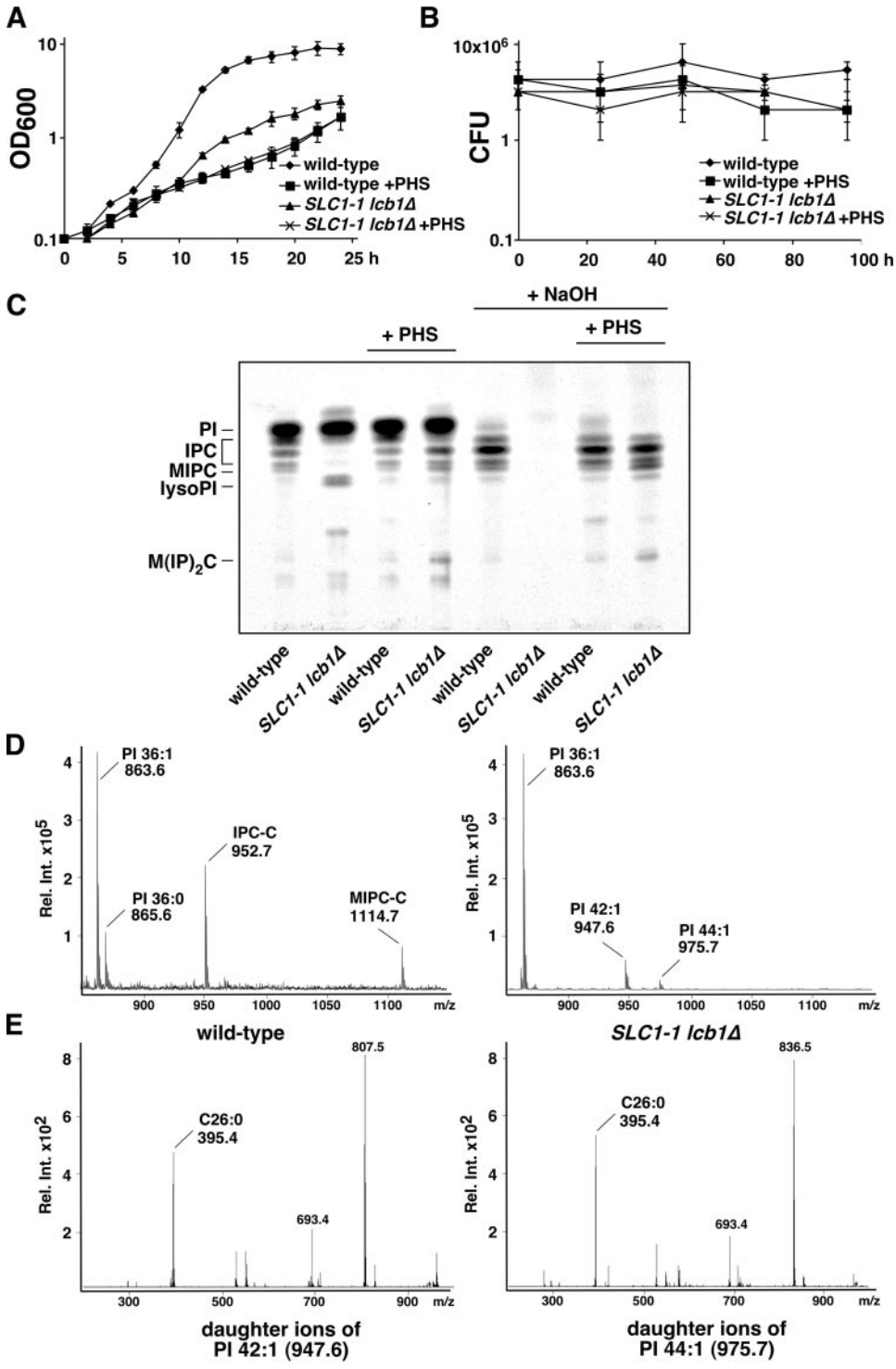


FIGURE 2. The *SLC1-1* strain grows and is viable in the absence of sphingolipids. *A*, comparison of growth rates between wild-type (YRS1878) and *SLC1-1 lcb1Δ* (YRS1877) suppressor strain in the absence or presence (+PHS) of phytosphingosine. Cells were cultivated in complete synthetic liquid medium at 24 °C, and optical density was recorded over time. *B*, comparison of colony formation capacity between wild-type and *SLC1-1* suppressor strain. Cells were cultivated in complete synthetic liquid medium at 24 °C, and aliquots were removed at the times indicated, diluted, and plated on solid YPD medium. Colonies were counted after 4 days of incubation at 24 °C. Values given in *A* and *B* represent means and S.D. of two independent determinations. *C*, comparison of inositol-containing lipids between wild-type and *SLC1-1* suppressor strain. Cells were cultivated in the absence or presence of PHS, and lipids were labeled with [³H]inositol, extracted, and analyzed by TLC. Mild base-resistant sphingolipids are shown on the right half of the chromatogram. Lipids are indicated as follows. PI, phosphatidylinositol; IPC, inositolphosphorylceramide; lysoPI, lysophosphatidylinositol; MIPC, mannosyl-inositolphosphorylceramide; and M(IP)₂C, mannosyl-diinositolphosphorylceramide. *D*, analysis of suppressor lipids by mass spectrometry. Microsomal membranes were prepared from wild type and the *SLC1-1 lcb1Δ* suppressor strain, and lipids were extracted and analyzed by mass spectrometry. Sphingolipids in wild-type cells are IPC-C (*m/z* 952.7) and MIPC-C (*m/z* 1114.7). C26 containing glycerophosphoinositol species in *SLC1-1 lcb1Δ* are PI 42:1 (*m/z* 947.6) and PI 44:1 (*m/z* 975.7). *E*, suppressor lipids contain a C26:0 fatty acid. Fragmentation of the suppressor lipids PI 42:1 (*m/z* 947.6) and PI 44:1 (*m/z* 975.7) reveals daughter ions of *m/z* 395.4 corresponding to C26:0. CFU, colony-forming units.

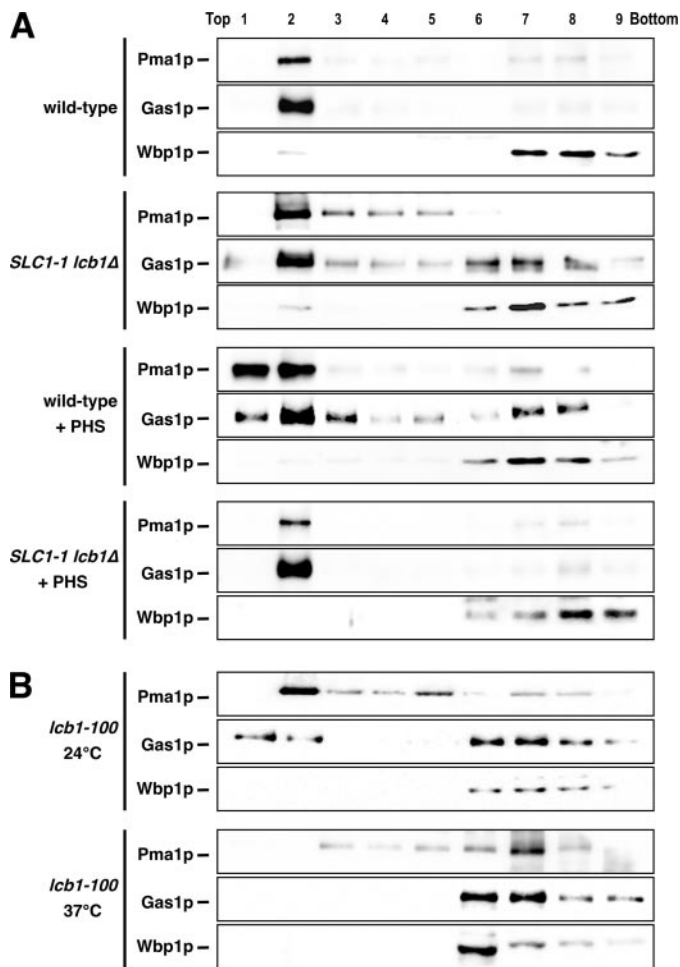


FIGURE 3. Steady-state association of Pma1p and Gas1p with detergent-resistant membranes in the absence of sphingolipids. *A*, wild type (YRS1878) and the *SLC1-1 lcb1Δ* (YRS1877) suppressor strain were cultivated at 24 °C in liquid synthetic medium in the presence or absence of PHS to early logarithmic growth phase. Membranes were extracted with Triton X-100 and floated in an Optiprep gradient. Fractions were collected from the top of the gradient, and proteins were precipitated by trichloroacetic acid and analyzed on Western blots probed with antisera against Pma1p, Gas1p, and the ER membrane protein Wbp1p. *B*, the association of Pma1p and Gas1p with detergent-resistant membranes depends on the synthesis of sphingolipids. *lcb1-100* (YRS1029) was cultivated at 24 °C and split, and half of the culture was shifted to 37 °C for 4 h. Membranes were extracted with detergent, fractionated on an Optiprep gradient, and analyzed by Western blot.

tant membrane fraction even in cells lacking sphingolipids but making suppressor lipids (Fig. 3A). The ER membrane protein and component of the oligosaccharyltransferase complex, Wbp1p, on the other hand, was solubilized upon detergent treatment and stayed in the bottom fractions of the gradient. Depletion of sphingolipids by using a temperature-sensitive mutant in long-chain base synthesis, *lcb1-100* (*end8-1*), impaired the association of Pma1p and Gas1p with detergent-resistant membranes at the nonpermissive temperature, as has been observed before (20, 25) (Fig. 3B). These results thus indicate that the function of sphingolipids in the formation of detergent-resistant membrane domains at the plasma membrane can be substituted by C26-containing inositol glycerophospholipids made in the *SLC1-1* suppressor strain. This substitution, however, appears to be slightly compromised, as indicated by the fact that the flotation behavior of both Pma1p

and Gas1p when isolated from the *SLC1-1* suppressor strain differs slightly from that of wild-type cells. When isolated from the suppressor strain, Pma1p and Gas1p displayed a trailing population of protein that did not exclusively fractionate in the top fraction, as was the case in wild type. Similarly, the addition of PHS to wild-type cells induced the appearance of a population of Gas1p that was detergent-soluble. PHS addition has previously been shown to induce ubiquitin-dependent internalization and down-regulation of the uracil permease Fur4p (26). Based on this observation, it is conceivable that PHS also induces down-regulation of Gas1p and that this down-regulation is accompanied by the exclusion of Gas1p from detergent-resistant membranes.

Suppressor Lipids Functionally Substitute Sphingolipids in Surface Transport of Newly Synthesized Pma1p—Sphingolipid synthesis is required for the association of newly synthesized Pma1p with detergent-resistant membranes already in the ER and for proper routing of Pma1p to the cell surface (2, 7, 8). In the absence of sphingolipids, newly synthesized Pma1p is rapidly degraded in the vacuole. Given that C26-containing suppressor lipids can substitute for sphingolipids in raft association of steady-state levels of Pma1p at the plasma membrane, we examined whether these lipids also protected newly synthesized Pma1p from missorting to the vacuole. Therefore, the stability of newly synthesized Pma1p in the *SLC1-1* suppressor strain grown in the presence or absence of PHS was examined by pulse-chase analysis and immunoprecipitation. These experiments revealed that newly synthesized Pma1p was stable in the *SLC1-1* suppressor strain independent of whether suppressor lipids or sphingolipids were synthesized (Fig. 4A). This result would thus indicate that suppressor lipids functionally substitute for sphingolipids also in surface transport of newly synthesized Pma1p. Moreover, the suppressor lipids appeared to provide full functionality as indicated by the fact that Pma1p was stable even when synthesized at 37 °C. The stability of Pma1p at 37 °C allows for discrimination between fully functional sphingolipids with a mature C26 fatty acid and those that are conditionally impaired in function due to the presence of a C22 fatty acid, as is the case in acyl chain elongase mutant cells, *elo3Δ* (10, 11, 27).

Given that suppressor lipids can substitute for sphingolipids in surface transport of Pma1p, one would expect that Pma1p biogenesis in the suppressor strain becomes resistant against degradation induced by drugs that inhibit sphingolipid biosynthesis. To test this prediction, we compared the stability of newly synthesized Pma1p in the *SLC1-1* strain with that of wild-type cells upon treatment with three different inhibitors of the sphingolipid biosynthetic pathway. Myriocin (20 μg/ml) was used to block long-chain base synthesis by serine palmitoyltransferase, fumonisin B1 (72 μg/ml) to block ceramide synthase, and aureobasidin A (2 μg/ml) to inhibit the conversion of ceramide to inositolphosphorylceramide (28–30). This analysis revealed that Pma1p was rapidly turned over in drug-treated wild-type cells but that Pma1p was stable in the *SLC1-1* suppressor strain (Fig. 4B). This observation is thus consistent with the notion that the C26-containing suppressor lipids functionally substitute for sphingolipids in surface transport of newly synthesized Pma1p. In addition, these data indi-

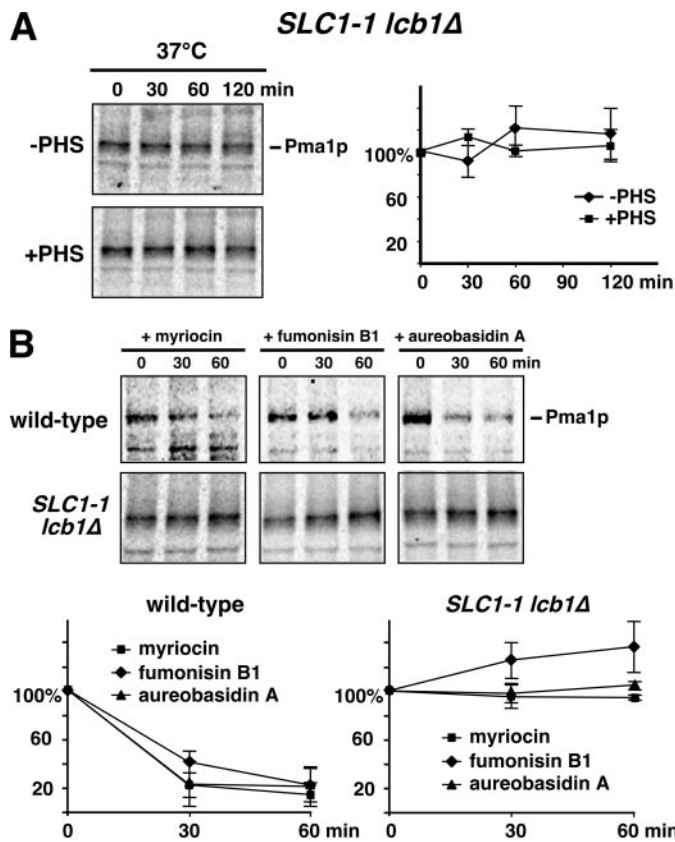


FIGURE 4. Newly synthesized Pma1p is stable and resistant against sphingolipid-dependent turnover in *SLC1-1*. *A*, *SLC1-1 lcb1Δ* (YRS1877) was cultivated in liquid synthetic medium with or without PHS at 24 °C and shifted to 37 °C for 15 min, and Pma1p stability was examined by pulse-chase analysis and immunoprecipitation. Levels of Pma1p were quantified using a PhosphorImager and are shown in the graph. *B*, biogenesis of Pma1p in the suppressor strain is resistant against sphingolipid-dependent degradation. Wild-type (YRS1878) and *SLC1-1 lcb1Δ* (YRS1877) suppressor cells were cultivated at 24 °C; preincubated with either myriocin (20 μg/ml), fumonisin B1 (75 μg/ml), or aureobasidin A (2 μg/ml) for 15 min; and then shifted to 37 °C for 15 min. Cells were labeled, and Pma1p turnover was examined by immunoprecipitation. Quantification of Pma1p levels is shown in the graph. The data shown in *A* and *B* represent means and S.D. of three independent experiments.

cate that surface transport of Pma1p is one of the essential pathways that is blocked by these three inhibitors of the sphingolipid pathway in wild-type cells.

To confirm that Pma1p reaches the cell surface in the absence of sphingolipids rather than stably accumulating within an intracellular compartment, we examined the steady-state distribution of a GFP-tagged version of Pma1p by fluorescent microscopy. In cells lacking sphingolipids, Pma1p-GFP displayed a characteristic ringlike staining at the cell periphery, consistent with surface transport of Pma1p in the absence of sphingolipids. No fluorescence was observed to accumulate in the vacuole, even in *SLC1-1* cells that were shifted to 37 °C, indicating that Pma1p is stable at the cell surface in the absence of sphingolipids (Fig. 5). Drug-induced inhibition of sphingolipid synthesis resulted in vacuolar localization of Pma1p-GFP in wild-type cells but not in the *SLC1-1* suppressor strain (Fig. 5). Taken together, these results indicate that the C26-containing suppressor lipids that are synthesized in the semidominant 1-acyl-*sn*-glycerol-3-phosphate acyltransferase mutant *SCL1-1*

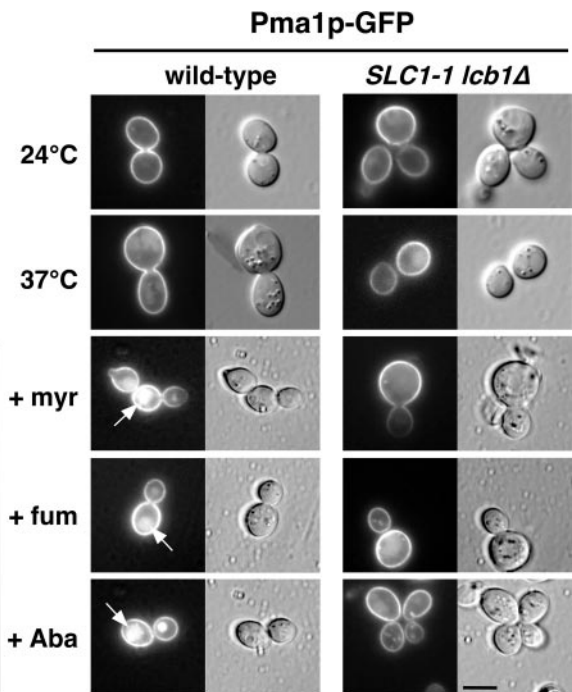


FIGURE 5. Steady-state localization of Pma1p to the cell surface in *SLC1-1* is resistant against sphingolipid-dependent turnover. Pma1p is located at the plasma membrane in the absence of sphingolipids. Wild-type (YRS2569) and *SLC1-1 lcb1Δ* (YRS2941) expressing a GFP-tagged version of Pma1p were cultivated in liquid synthetic medium at 24 °C or shifted to 37 °C for 2 h in the presence or absence of sphingolipid inhibitors (myriocin (*myr*) (20 μg/ml), fumonisin B1 (*fum*) (75 μg/ml), and aureobasidin A (*Aba*) (2 μg/ml)), and the subcellular localization of Pma1p was examined by fluorescence microscopy. Bar, 5 μm.

strain fully substitute for sphingolipids in surface transport and stabilization of Pma1p.

Long-chain Base Synthesis Is Dispensable for Endocytosis in the Suppressor Strain—Long-chain base synthesis is required for the internalization step of endocytosis and for the organization of the actin cytoskeleton (31). We previously showed that the accelerated turnover of Pma1p in an *elo3Δ* mutant at 37 °C can be rescued by preventing endocytosis, indicating that turnover of Pma1p in *elo3Δ* occurs after the protein has reached the cell surface (10). To examine whether the apparent stability of newly synthesized Pma1p in the suppressor strain was due to a block in endocytosis in this strain, we examined whether the suppressor strain was defective in endocytosis. Uptake of the fluid phase marker lucifer yellow in the *SLC1-1* strain, however, was comparable with that of wild-type cells, and the fluorescent dye was rapidly transported to the vacuole, indicating that endocytosis is functional even in the absence of sphingolipids (Fig. 6A). A block in *de novo* sphingolipid biosynthesis using the conditional *lcb1-100* mutant, on the other hand, resulted in a block in endocytosis in cells incubated at 37 °C, and this block was rescued by the addition of PHS, consistent with the reported requirement for long-chain base synthesis in endocytosis in cells that make sphingolipids (31). The long-chain base requirement for endocytosis can be overcome by overexpression of protein kinases (*YCK2*, *PKC1*, and *PKH1/2*) or inactivation of the ceramide-activated *PP2A* (protein phosphatase 2A) (32, 33). The fact that the suppressor strain has no block in endocytosis is interesting and may be explained by the absence

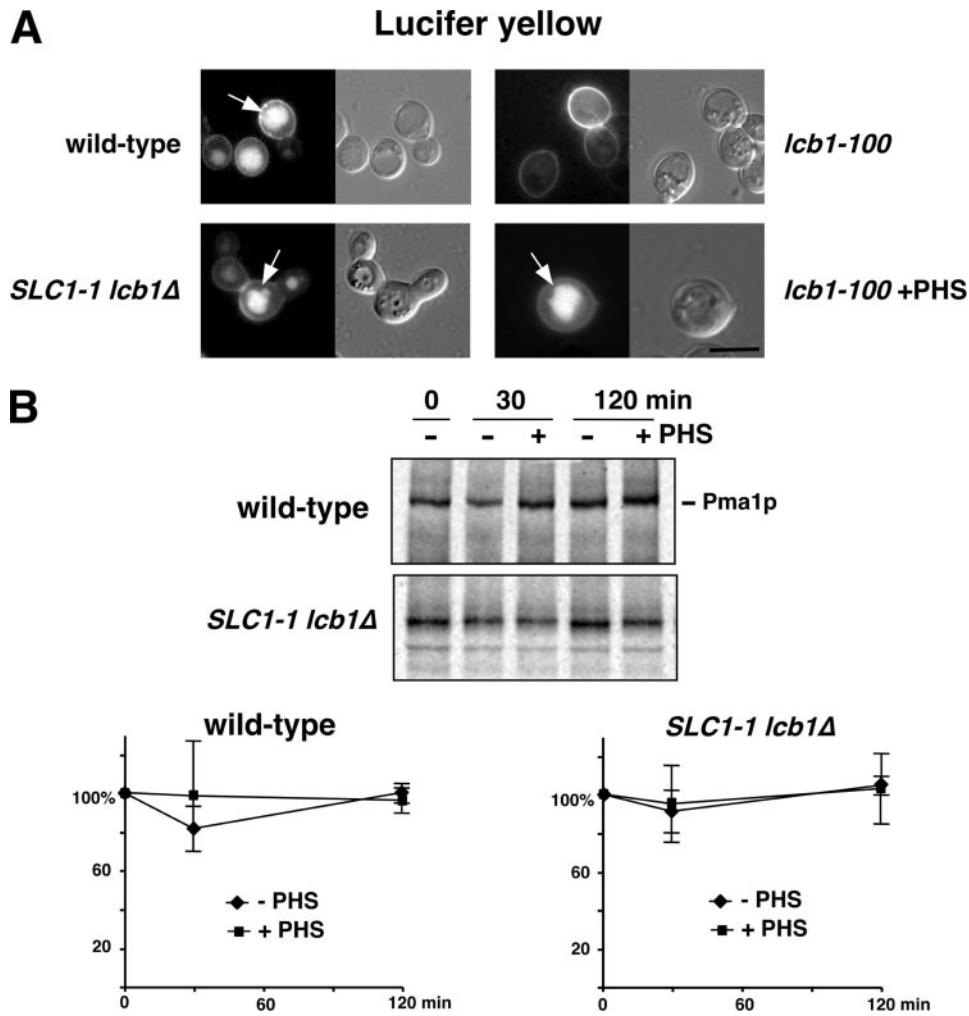


FIGURE 6. A block in endocytosis does not account for the apparent stability of Pma1p in *SLC1-1*. *A*, endocytosis of lucifer yellow in the suppressor strain is not affected by the absence of sphingolipids. Wild-type (YRS1878), *SLC1-1 lcb1Δ* (YRS1877), and *lcb1-100* (YRS1029) cells were cultivated in liquid synthetic medium lacking or containing PHS (+PHS; 25 μ M) at 24 °C and shifted to 37 °C for 2 h. Cells were incubated with lucifer yellow (5 mg/ml) for 60 min at 37 °C and analyzed by fluorescence microscopy. Delivery of lucifer yellow to the vacuole is indicated by arrows. Bar, 5 μ m. *B*, Pma1p stability in *SLC1-1 lcb1Δ* is not affected by the addition of PHS. Wild-type and *SLC1-1 lcb1Δ* were cultivated in liquid synthetic medium at 24 °C, shifted to 37 °C for 2 h, pulse-labeled at time 0 for 15 min, and chased for 30 and 120 min in the presence or absence of PHS (25 μ M) that was added at time 0. Quantification of Pma1p levels is shown in the graphs. The data shown represent means and S.D. of three independent experiments.

of ceramide and hence reduced PP2A activity in these cells, thus allowing endocytosis to proceed in the absence of a long-chain base.

To confirm that the apparent stability of newly synthesized Pma1p in the suppressor strain was not due to a defect in PHS-dependent endocytosis, we examined the stability of Pma1p by pulse-chase analysis in the presence or absence of PHS, added at the beginning of the labeling period. Samples were then taken 30 or 120 min after PHS addition, and Pma1p levels were determined by immunoprecipitation. If PHS were required for endocytosis in the *SLC1-1* strain, one would predict that its addition would ultimately result in down-regulation of Pma1p. The addition of PHS, however, did not affect Pma1p levels in the suppressor strain (Fig. 6B). This observation is thus consistent with the notion that the stability of Pma1p in this suppressor strain is not due to a defect in endocytosis and vacuolar degra-

ation of the protein but reflects stable delivery of Pma1p to the plasma membrane in the absence of sphingolipids.

Suppressor Lipids Functionally Substitute Sphingolipids in Raft Association of Newly Synthesized Pma1p—Newly synthesized Pma1p rapidly acquires detergent resistance in wild-type cells, and we previously showed that this is independent of ongoing sterol synthesis but that raft association of Pma1p depends on the presence of a mature C26 fatty acid on sphingolipids, because an acyl chain elongase mutant, *elo3Δ*, conditionally affects detergent association of Pma1p at 37 °C (2, 11). To determine whether suppressor lipids provided detergent resistance to newly made Pma1p, we examined detergent solubility of newly synthesized Pma1p by pulse-chase analysis and immunoprecipitation. This type of analysis is performed in cells that lack the vacuolar protease Pep4p and hence do not degrade newly made Pma1p upon mistargeting to the vacuole (10, 11). Pulse-chase analysis followed by detergent extraction revealed that newly synthesized Pma1p acquired detergent resistance in *pep4Δ* mutant cells that lacked sphingolipids but synthesized suppressor lipids (Fig. 7). The kinetics with which Pma1p became detergent-resistant, however, appeared to be slowed in the *SLC1-1* strain (*SLC1-1 lcb1Δ pep4Δ*) compared with wild type (*pep4Δ*). This was particularly evi-

dent at 24 °C. Nevertheless, the fact that Pma1p acquired detergent resistance even at 37 °C indicated that suppressor lipids were functional even under high stringent conditions. Suppressor lipids thus are more functional in supporting biogenesis of Pma1p than are sphingolipids having a shortened C22 fatty acid, as made in the acyl chain elongase mutant, *elo3Δ*.

The Essential Functionality of Suppressor Lipids Depends on the Presence of the C26 Fatty Acid—Having established the functionality of suppressor lipids in raft association and stable surface transport of Pma1p, we next asked whether the function of these lipids required the presence of the mature C26 acyl chain or whether a shorter C22 acyl chain would still provide functionality to these suppressor lipids. Therefore, we generated a *SLC1-1 lcb1Δ elo3Δ* mutant strain in which the suppressor lipids are expected to carry a C22 rather than a C26 fatty acid. Remarkably, this strain was viable only when supple-

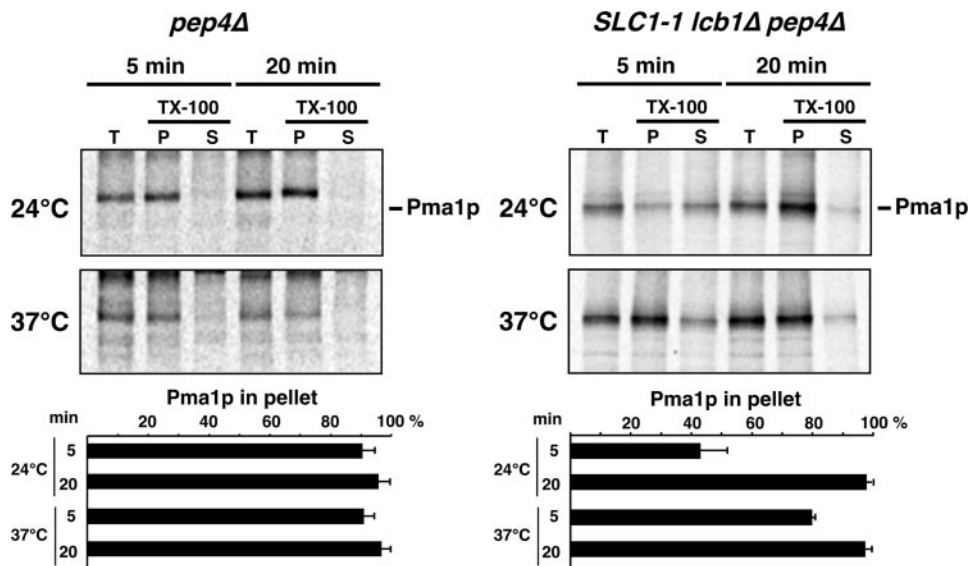


FIGURE 7. Newly synthesized Pma1p rapidly acquires detergent resistance in *SLC1-1. pep4Δ*-deficient wild-type (YRS2843) and *SLC1-1 lcb1Δ* (YRS2138) cells were pulse-labeled at either 24 °C or after a preshift to 37 °C for 15 min. Samples were removed at the indicated time points after the addition of chase and split into a total (T) fraction and a second fraction that was extracted with 1% Triton X-100 for 30 min on ice. The detergent fraction was centrifuged at $100,000 \times g$ for 1 h to yield a detergent-resistant pellet (P) and a soluble (S) fraction. Pma1p was immunoprecipitated and analyzed by gel electrophoresis. Quantification of Pma1p levels in the detergent-resistant pellet as a function of temperature and time is shown in the graphs, in which the signal intensity obtained in the total fraction (T) was set to 100%, and that of the detergent-resistant pellet (P) is represented as a black bar. The data shown represent means and S.D. values of three independent experiments.

mented with PHS, indicating that the essential functionality of suppressor lipids indeed critically depended on the presence of the mature C26 fatty acid (Fig. 8A). When cultivated in liquid medium lacking PHS, the strain ceased growth after ~12 h of growth, a time point at which endogenous PHS levels probably became depleted (Fig. 8B). Analysis of Pma1p stability in this *SLC1-1 lcb1Δ elo3Δ* mutant strain revealed rapid turnover and delivery of Pma1p to the vacuole at 37 °C, independent of the presence or absence of PHS (Fig. 8, C and D). These results thus indicated that the *SLC1-1 lcb1Δ elo3Δ* mutant strain displayed the same conditional turnover of Pma1p as observed in the elongase, *elo3Δ*, mutant itself. These observations thus strongly indicate that the mature C26 fatty acid either bound to a ceramide or a glycerophospholipid is critical for stable surface delivery of Pma1p at 37 °C, consistent with our earlier observations (10, 11). The C26 acyl chain on suppressor lipids thus is essential, and one of the essential functions that these very long acyl chains fulfill is to promote surface transport and stabilization of the proton-pumping ATPase.

DISCUSSION

The aim of this study was to discriminate between the role of ceramide/sphingolipids and that of the saturated very long-chain C26 fatty acid that is present on the yeast ceramide in promoting raft association and stable surface transport of the plasma membrane H^+ -ATPase, Pma1p. To discriminate between the function of ceramide and that of the C26 very long-chain fatty acid, which under normal conditions (*i.e.* in sphingolipid-synthesizing cells) are intimately related, we made use of a suppressor strain that synthesizes C26-containing inositolphospholipids instead of sphingolipids due to the pres-

ence of a semidominant mutation in a 1-acyl-*sn*-glycerol-3-phosphate acyltransferase, *SLC1-1* (15).

Characterization of this suppressor strain revealed that the C26-containing inositolphospholipids robustly substituted for sphingolipids in all of the aspects tested. (i) Suppressor lipids substituted for sphingolipids in raft association of steady-state levels of Pma1p and Gas1p at the yeast plasma membrane. (ii) Suppressor lipids enabled newly synthesized Pma1p to rapidly acquire detergent resistance. (iii) They promoted routing of Pma1p to the cell surface. (iv) They promoted stabilization at the surface. These results thus indicate that the C26 fatty acid rather than ceramide or sphingolipids *per se* provides the important function of sphingolipids in Pma1p biogenesis.

In addition to being functional in transport and stabilization of Pma1p, suppressor lipids also allow the H^+ -ATPase to be enzymatically

active at the plasma membrane, since loss of Pma1p function would be lethal (34). The efficiency of proton extrusion by the H^+ -ATPase in the absence of sphingolipids, however, is limiting, as indicated by the fact that cells with suppressor lipids are unable to grow at low pH, at 37 °C, or in the presence of high salt concentrations (34). These environmental stresses are known to inhibit the growth of strains with defective H^+ -ATPase, indicating that the efficiency of Pma1p in the absence of sphingolipids is compromised. Whether sphingolipids are directly required for the enzymatic function of Pma1p or whether the reduced proton extrusion that is observed in the suppressor strain is due to an impaired proton permeability barrier of a membrane without sphingolipids, however, remains to be determined (34).

Consistent with the notion that the C26 fatty acid provides the important function of sphingolipids in Pma1p biogenesis, we find that the function of suppressor lipids in Pma1p biogenesis and possibly other vital functions critically depends on the presence of the C26 fatty acid. This is indicated by the fact that the suppressor strain is not viable in combination with a mutation that results in the synthesis of shorter acyl chains, *elo3Δ*. These results thus strongly indicate that the conditional turnover of Pma1p observed in *elo3Δ* mutant cells is due to a structural role of C26-containing sphingolipids rather than a possible signaling function of intermediates of the sphingolipid pathway, such as long-chain base or ceramide. In addition, the results also indicate that at least one essential function of sphingolipids is provided by the ceramide-bound C26 fatty acid (*i.e.* the biogenesis of the essential Pma1p).

C26-containing lipids are a hallmark of the yeast plasma membrane. Synthesis of these lipids, however, occurs in the ER,

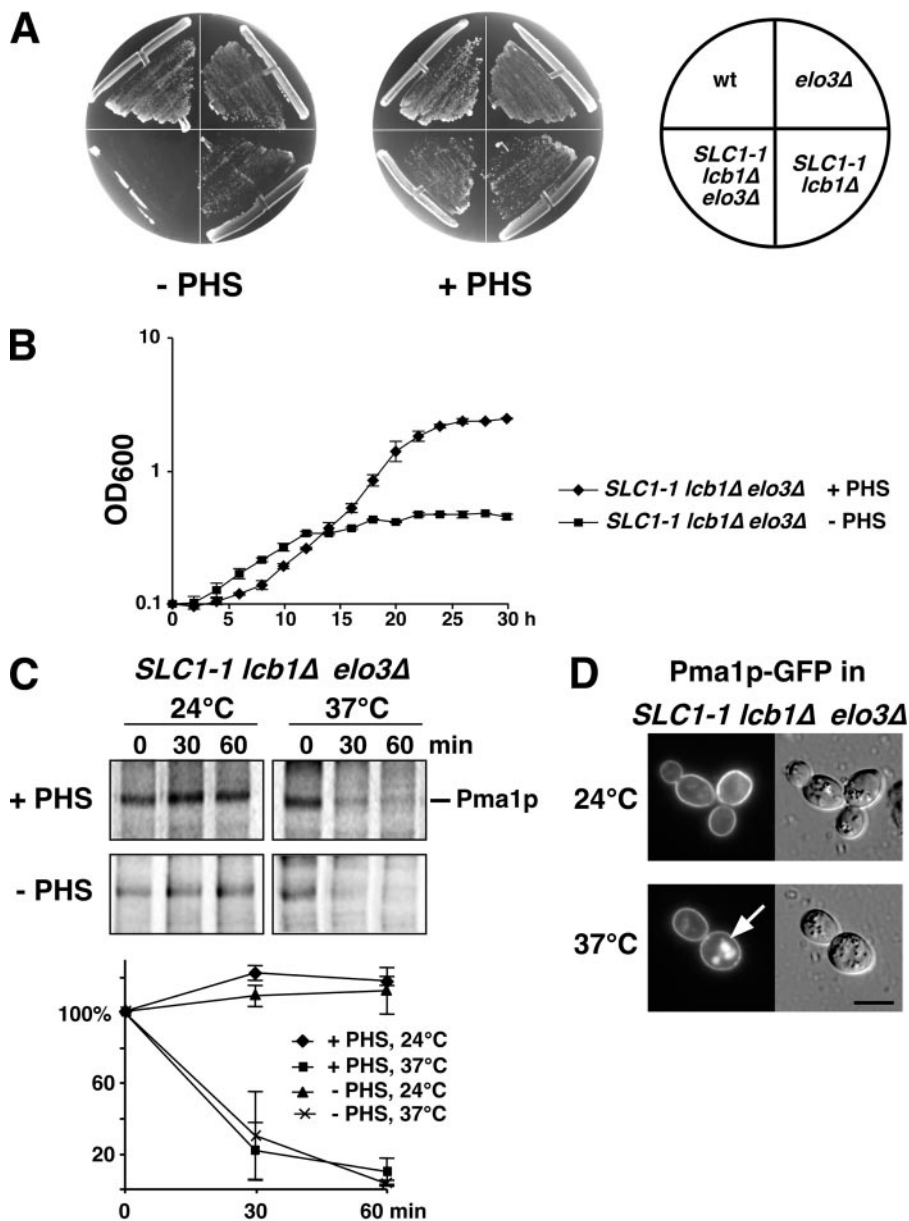


FIGURE 8. Suppressor lipids require a C26 fatty acid for functionality. *A*, viability of a suppressor strain combined with a mutation in the elongase (*ELO3*) depends on exogenous PHS. Wild-type (YRS1878) *elo3Δ* (YRS1118), *SLC1-1 lcb1Δ* (YRS1877), and *SLC1-1 lcb1Δ elo3Δ* (YRS2914) cells were streaked onto solid synthetic medium containing or lacking PHS (5 μ M). Growth was recorded after 4 days of incubation at 24 °C. *B*, comparison of growth rates of *SLC1-1 lcb1Δ elo3Δ* (YRS2914) in the absence or presence (+PHS) of phytosphingosine. Cells were cultivated in complete synthetic liquid medium at 24 °C, and optical density was recorded over time. Values represent means and S.D. values of two independent determinations. *C*, conditional turnover of newly synthesized Pma1p in a *SLC1-1 lcb1Δ elo3Δ*. The suppressor strain lacking *ELO3* (YRS2914) was cultivated in the presence of PHS or shifted to medium lacking PHS for 6 h and incubated at either 24 or 37 °C for 15 min. Pma1p stability was examined by pulse-chase analysis and immunoprecipitation. Quantification of Pma1p levels is shown in the graph. The data shown represent means and S.D. of three independent experiments. *D*, Pma1p-GFP reaches the vacuole in the suppressor strain lacking *ELO3*. The suppressor strain lacking *ELO3* expressing Pma1p-GFP (YRS2943) was cultivated in the medium supplemented with PHS (5 μ M) at 24 °C. Cells were shifted to 37 °C for 2 h and analyzed by fluorescence microscopy. Vacuolar staining is indicated by an arrow. Bar, 5 μ m.

where both the fatty acid elongase and the ceramide synthase are located (35, 36). Thus, similar to integral membrane proteins that are destined to the cell surface, C26-containing ceramide/sphingolipids must travel from the ER to the plasma membrane. The fact that these lipids affect detergent solubility of newly synthesized Pma1p already upon ER exit would indicate that lipids and proteins may already assemble at their site

of synthesis and are then cotransported to the surface (2). A failure to properly assemble this lipid-protein complex results either in a diversion of surface-destined vesicle to the vacuole, a failure to stabilize the complex upon arrival at the plasma membrane, or both (7–10).

Our observations indicate that C26-containing lipids are essential for the formation of functional lipid-protein complexes. The precise function that the C26 acyl chain fulfills in this assembly, however, remains to be defined. It has been suggested that the length of the transmembrane domain of proteins along the secretory pathway may increase to match bilayers of increasing “thickness” (37). In such a model, the abundance of C26-containing lipids may determine the thickness of membranes along the secretory pathway. The evidence that the yeast plasma membrane is thicker than other membranes, however, is mostly based on electron microscopy and thus susceptible to possible artifacts based on the fixation and staining procedures (38, 39). Biophysical studies with pure lipid bilayers indicate that lipids with highly asymmetric acyl chains can interdigitate into the hydrophobic core of the opposite half of the bilayer and thus do not necessarily increase the thickness of the bilayer (40, 41). Such studies, however, do not account for the role of sterols, proteins, and an asymmetric lipid composition of the two leaflets of the bilayer on the precise arrangement of the very long acyl chains and their effects on the bilayer. Proteins, for example, have recently been shown to modulate bilayer thickness by more than 10% (42). The thickness of the lipid component of a biological membrane thus must not naturally match that of the proteins as has been suggested before (43, 44).

Based on these considerations, we believe that it is premature to correlate acyl chain length with bilayer thickness in biological membranes and that an alternative function of the C26 acyl chains could be to interdigitate into the opposite leaflet, thereby (i) coupling the two halves of the bilayer to lower the energy required to deform this potentially stiff cholesterol-rich membrane and (ii) increasing acyl

chain packing density to prevent permeability by small molecules, particularly protons.

The ceramide backbone and saturated acyl chain on sphingolipids favorably interact with sterols to form condensed complexes that are generally believed to be a driving force for microdomain formation (14, 45). The fact that the ceramide backbone on the yeast sphingolipids is dispensable for the function of sphingolipids in Pma1p biogenesis is in agreement with our previous observation that Pma1p biogenesis is independent of the precise sterol structure and even independent of ongoing sterol synthesis (11). Genetic interactions between mutations in acyl chain elongation and defects in certain sterol modifications, on the other hand, indicate that, *in vivo*, sphingolipid-sterol interactions are affected by the length of the C26 acyl chain of sphingolipids (10).

A better understanding of the role that these asymmetrical C26-containing lipids have on protein sorting to the plasma membrane is important because elongase mutant cells not only affect Pma1p stability but also show delayed ER to Golgi transport of the glycosylphosphatidylinositol-anchored protein Gas1p and defective surface transport of an artificial membrane-anchored cargo protein (35, 46). We have previously characterized the biophysical properties of an inositol glycerophospholipid with a C26 fatty acid in position *sn*-1 and shown that this lipid is very potent in lowering the bilayer to hexagonal transition temperature of liposomes composed of DEPE (1,2-dielaidoyl-*sn*-glycero-3-phosphoethanolamine) (47). This observation is consistent with the proposition that this highly asymmetrical lipid could be important in stabilizing highly curved membrane structures. Although we currently do not know whether a phosphatidylinositol with a C26 acyl chain in position *sn*-2, as made in the *SLC1-1* suppressor strain, or a C26-containing ceramide would exhibit similar biophysical properties, it is tempting to speculate that the effect on membrane curvature is a general property of these highly asymmetrical lipids and that one of the essential functions these lipids may fulfill is to stabilize highly curved membrane domains that are transiently formed during vesicle budding and fusion along the secretory pathway (48). Biophysical experiments to compare the properties of such highly asymmetric lipids will hopefully be instructive to better define the function of these lipids *in vivo*.

Acknowledgments—We thank R. Dickson for making the suppressor strain available, Olivier Aebischer for help with mass spectrometry, and R. Tiwari for comments on the manuscript.

REFERENCES

- Behnia, R., and Munro, S. (2005) *Nature* **438**, 597–604
- Lee, M. C., Hamamoto, S., and Schekman, R. (2002) *J. Biol. Chem.* **277**, 22395–22401
- Roerg, K. J., Crotwell, M., Espenshade, P., Gimeno, R., and Kaiser, C. A. (1999) *J. Cell Biol.* **145**, 659–672
- Harsay, E., and Schekman, R. (2002) *J. Cell Biol.* **156**, 271–285
- Gurunathan, S., David, D., and Gerst, J. E. (2002) *EMBO J.* **21**, 602–614
- Malinska, K., Malinsky, J., Opekarova, M., and Tanner, W. (2003) *Mol. Biol. Cell* **14**, 4427–4436
- Wang, Q., and Chang, A. (2002) *Proc. Natl. Acad. Sci. U. S. A.* **99**, 12853–12858
- Bagnat, M., Chang, A., and Simons, K. (2001) *Mol. Biol. Cell* **12**, 4129–4138
- Gong, X., and Chang, A. (2001) *Proc. Natl. Acad. Sci. U. S. A.* **98**, 9104–9109
- Eisenkolb, M., Zenzmaier, C., Leitner, E., and Schneiter, R. (2002) *Mol. Biol. Cell* **13**, 4414–4428
- Gaigg, B., Timischl, B., Corbino, L., and Schneiter, R. (2005) *J. Biol. Chem.* **280**, 22515–22522
- Brown, D. A., and London, E. (1998) *Annu. Rev. Cell Dev. Biol.* **14**, 111–136
- Munro, S. (2003) *Cell* **115**, 377–388
- Simons, K., and Vaz, W. L. (2004) *Annu. Rev. Biophys. Biomol. Struct.* **33**, 269–295
- Lester, R. L., Wells, G. B., Oxford, G., and Dickson, R. C. (1993) *J. Biol. Chem.* **268**, 845–856
- Winzeler, E. A., Shoemaker, D. D., Astromoff, A., Liang, H., Anderson, K., Andre, B., Bangham, R., Benito, R., Boeke, J. D., Bussey, H., Chu, A. M., Connelly, C., Davis, K., Dietrich, F., Dow, S. W., El Bakkoury, M., Foury, F., Friend, S. H., Gentalen, E., Giaever, G., Hegemann, J. H., Jones, T., Laub, M., Liao, H., Liebundguth, N., Lockhart, D. J., Lucau-Danila, A., Lussier, M., M'Rabet, N., Menard, P., Mittmann, M., Pai, C., Rebischung, C., Revuelta, J. L., Riles, L., Roberts, C. J., Ross-MacDonald, P., Scherens, B., Snyder, M., Sookhai-Mahadeo, S., Storms, R. K., Veronneau, S., Voet, M., Volckaert, G., Ward, T. R., Wysocki, R., Yen, G. S., Yu, K., Zimmermann, K., Philippsen, P., Johnston, M., and Davis, R. W. (1999) *Science* **285**, 901–906
- Pinto, W. J., Srinivasan, B., Shepherd, S., Schmidt, A., Dickson, R. C., and Lester, R. L. (1992) *J. Bacteriol.* **174**, 2565–2574
- Balguer, A., Bagnat, M., Bonneu, M., Aigle, M., and Breton, A. M. (2002) *Eukaryot. Cell* **1**, 1021–1031
- Cross, F. R. (1997) *Yeast* **13**, 647–653
- Bagnat, M., Keranen, S., Shevchenko, A., and Simons, K. (2000) *Proc. Natl. Acad. Sci. U. S. A.* **97**, 3254–3259
- Dulic, V., Egerton, M., Elguindi, I., Raths, S., Singer, B., and Riezman, H. (1991) *Methods Enzymol.* **194**, 697–710
- Dickson, R. C., Wells, G. B., Schmidt, A., and Lester, R. L. (1990) *Mol. Cell Biol.* **10**, 2176–2181
- Dickson, R. C., and Lester, R. L. (2002) *Biochim. Biophys. Acta* **1583**, 13–25
- Nagiec, M. M., Wells, G. B., Lester, R. L., and Dickson, R. C. (1993) *J. Biol. Chem.* **268**, 22156–22163
- Sutterlin, C., Horvath, A., Gerold, P., Schwarz, R. T., Wang, Y., Dreyfuss, M., and Riezman, H. (1997) *EMBO J.* **16**, 6374–6383
- Chung, N., Jenkins, G., Hannun, Y. A., Heitman, J., and Obeid, L. M. (2000) *J. Biol. Chem.* **275**, 17229–17232
- Oh, C. S., Toke, D. A., Mandala, S., and Martin, C. E. (1997) *J. Biol. Chem.* **272**, 17376–17384
- Horvath, A., Sutterlin, C., Manning-Krieg, U., Movva, N. R., and Riezman, H. (1994) *EMBO J.* **13**, 3687–3695
- Merrill, A. H., Jr., van Echten, G., Wang, E., and Sandhoff, K. (1993) *J. Biol. Chem.* **268**, 27299–27306
- Nagiec, M. M., Nagiec, E. E., Baltisberger, J. A., Wells, G. B., Lester, R. L., and Dickson, R. C. (1997) *J. Biol. Chem.* **272**, 9809–9817
- Zanolari, B., Friant, S., Funato, K., Sutterlin, C., Stevenson, B. J., and Riezman, H. (2000) *EMBO J.* **19**, 2824–2833
- Friant, S., Zanolari, B., and Riezman, H. (2000) *EMBO J.* **19**, 2834–2844
- Friant, S., Lombardi, R., Schmelzle, T., Hall, M. N., and Riezman, H. (2001) *EMBO J.* **20**, 6783–6792
- Patton, J. L., Srinivasan, B., Dickson, R. C., and Lester, R. L. (1992) *J. Bacteriol.* **174**, 7180–7184
- David, D., Sundarababu, S., and Gerst, J. E. (1998) *J. Cell Biol.* **143**, 1167–1182
- Barz, W. P., and Walter, P. (1999) *Mol. Biol. Cell* **10**, 1043–1059
- Levine, T. P., Wiggins, C. A., and Munro, S. (2000) *Mol. Biol. Cell* **11**, 2267–2281
- Grove, S. N., Bracker, C. E., and Morre, D. J. (1968) *Science* **161**, 171–173
- Schneiter, R., Brügger, B., Sandhoff, R., Zellnig, G., Leber, A., Lampl, M.,

- Athenstaedt, K., Hrastnik, C., Eder, S., Daum, G., Paltauf, F., Wieland, F. T., and Kohlwein, S. D. (1999) *J. Cell Biol.* **146**, 741–754
40. Hui, S. W., Mason, T. J., and Huang, C.-H. (1984) *Biochemistry* **23**, 5570–5577
41. Mattai, J., Sripada, P. K., and Shipley, G. G. (1987) *Biochemistry* **26**, 3287–3297
42. Mitra, K., Ubarretxena-Belandia, I., Taguchi, T., Warren, G., and Engelman, D. M. (2004) *Proc. Natl. Acad. Sci. U. S. A.* **101**, 4083–4088
43. Mouritsen, O. G., and Bloom, M. (1993) *Annu. Rev. Biophys. Biomol. Struct.* **22**, 145–171
44. Killian, J. A. (1998) *Biochim. Biophys. Acta* **1376**, 401–415
45. Ramstedt, B., and Slotte, J. P. (2002) *FEBS Lett.* **531**, 33–37
46. Proszynski, T. J., Klemm, R. W., Gravert, M., Hsu, P. P., Gloor, Y., Wagner, J., Kozak, K., Grabner, H., Walzer, K., Bagnat, M., Simons, K., and Walch-Solimena, C. (2005) *Proc. Natl. Acad. Sci. U. S. A.* **102**, 17981–17986
47. Schneider, R., Brugger, B., Amann, C. M., Prestwich, G. D., Epanand, R. F., Zellnig, G., Wieland, F. T., and Epanand, R. M. (2004) *Biochem. J.* **381**, 941–949
48. McMahon, H. T., and Gallop, J. L. (2005) *Nature* **438**, 590–596
49. Sütterlin, C., Doering, T. L., Schimmöller, F., Schröder, S., and Riezman, H. (1997) *J. Cell Sci.* **110**, 2703–2714